





Design of Scaffolds Based on Zinc-Modified Marine Collagen and Bilberry Leaves Extract-Loaded Silica Nanoparticles as Wound Dressings

Mihaela Deaconu ^{1,2}, Ana-Maria Prelipcean ³, Ana-Maria Brezoiu², Raul-Augustin Mitran⁴, Ana-Maria Seciu-Grama ², Cristian Matei², Daniela Berger ²

¹CAMPUS Research Institute, National University of Science and Technology Politehnica Bucharest, Bucharest, 060042, Romania; ²Faculty of Chemical Engineering and Biotechnologies, National University of Science and Technology Politehnica Bucharest, Bucharest, 011061, Romania; ³National Institute of R&D for Biological Sciences, Bucharest, 060031, Romania; ⁴'Ilie Murgulescu' Institute of Physical Chemistry, Romanian Academy, Bucharest, 060021, Romania

Correspondence: Daniela Berger, Faculty of Chemical Engineering and Biotechnologies, National University of Science and Technology Politehnica Bucharest, 1-7 Polizu Street, Bucharest, 011061, Romania, Email daniela.berger@upb.ro

Purpose: In this study, wound dressings were designed using zinc-modified marine collagen porous scaffold as host for wild bilberry (WB) leaves extract immobilized in functionalized mesoporous silica nanoparticles (MSN). These new composites were developed as an alternative to conventional wound dressings. In addition to the antibacterial activity of classic antibiotics, a polyphenolic extract could act as an antioxidant and/or an anti-inflammatory agent as well.

Methods: Wild bilberry leaves extract was prepared by ultrasound-assisted extraction in ethanol and its properties were evaluated by UV-Vis spectroscopy (radical scavenging activity, total amount of polyphenols, flavonoids, anthocyanins, and condensed tannins). The extract components were identified by HPLC, and the antidiabetic properties of the extract were evaluated via α -glucosidase inhibitory activity. Spherical MSN were modified with propionic acid or proline moieties by post-synthesis method and used as carriers for the WB leaves extract. The textural and structural features of functionalized MSN were assessed by nitrogen adsorption/desorption isotherms, small-angle XRD, SEM, TEM, and FTIR spectroscopy. The composite porous scaffolds were prepared by freeze drying of the zinc-modified collagen suspension containing WB extract loaded silica nanoparticles.

Results: The properties of the new composites demonstrated enhanced properties in terms of thermal stability of the zinc-collagen scaffold, without altering the protein conformation, and stimulation of NCTC fibroblasts mobility. The results of the scratch assay showed contributions of both zinc ions from collagen and the polyphenolic extract incorporated in functionalized silica in the wound healing process. The extract encapsulated in functionalized MSN proved enhanced biological activities compared to the extract alone: better inhibition of *P. aeruginosa* and *S. aureus* strains, higher biocompatibility on HaCaT keratinocytes, and anti-inflammatory potential demonstrated by reduced IL-1 β and TNF- α levels.

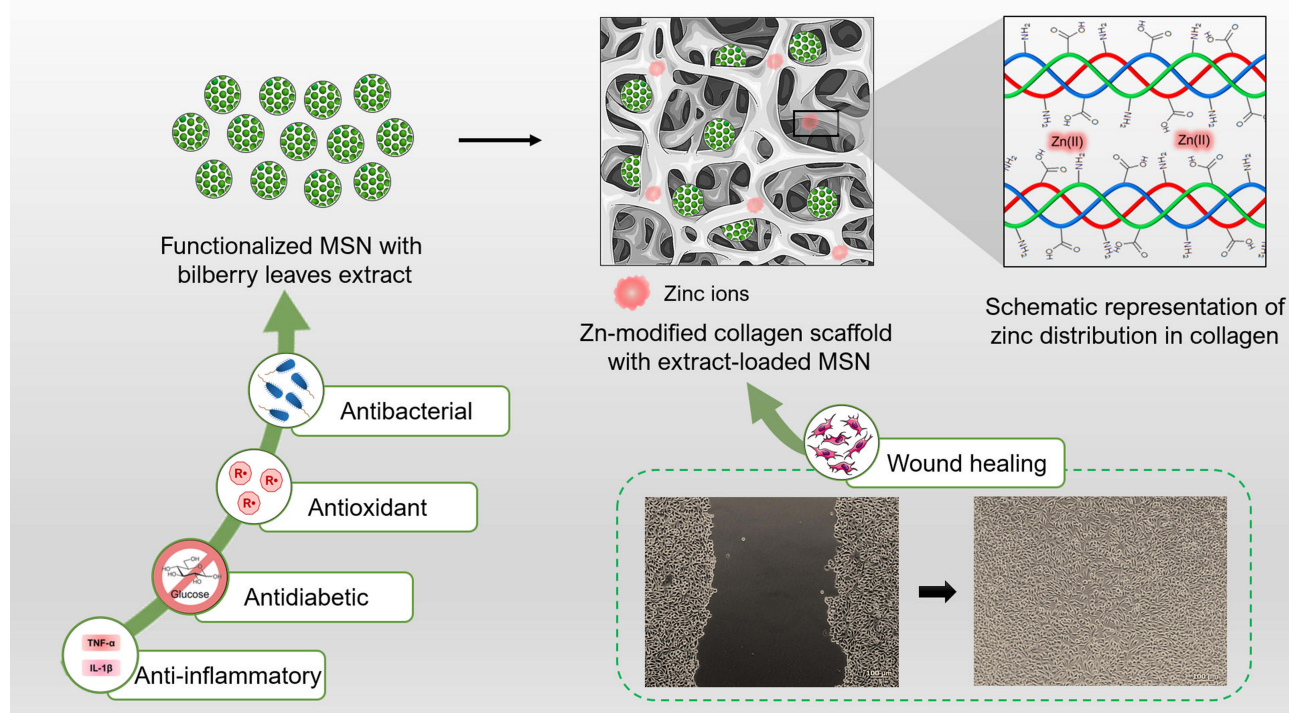
Conclusion: The experimental data shows that the novel composites can be used for the development of effective wound dressings.

Keywords: mesoporous silica carrier, bilberry leaves extract, marine collagen, antibacterial composite, anti-inflammatory activity

Introduction

Thermal injuries cause skin damage that can become a challenge for patients because the wound healing process is complex and it requires approaches that target not only skin regeneration, but also other issues, like microbial contamination and scar formation. Wound dressings are a barrier against bacterial contamination, however through tissue engineering, these dressings have become complex tools that serve as more than just a cover for the wound, they also assist in the healing process. The materials used in the design of commercially available wound dressings often include synthetic polymers. However, natural polymers, like chitosan,¹ alginate,² or collagen,³ are more favorable

Graphical Abstract



because their obtaining does not require organic solvents, and they have high biocompatibility. Among these naturally occurring polymers, collagen seems to be the most promising in terms of biocompatibility, since it is a major tissue component.³

Collagen sponges obtained from terrestrial mammals like bovine, porcine or equine sourced collagen were approved by FDA as wound dressings for various clinical indications.⁴ Modification of collagen matrices can improve the physico-chemical characteristics, ie, their thermal stability. A common technique to improve thermal stability of collagen matrix is crosslinking through chemical or physical treatment. However, most often these methods require the use of chemical reagents, ie, glutaraldehyde, which has toxicity issues, or it can cause the disruption of collagen triple helical structure.⁴ The introduction of low concentration of Cu^{2+} or Zn^{2+} ions does not affect the secondary structure of collagen⁵ and enhances its thermal stability.⁶ Furthermore, Ca^{2+} , Zn^{2+} , Mg^{2+} , Fe^{3+} or Cu^{2+} ions influence different stages of wound healing process.⁷⁻⁹ Among these, zinc stimulates skin cells motility and has anti-inflammatory properties.¹⁰

Recent reports highlight the preventive potential of compounds obtained from vegetal sources in the evolution of different disorders.¹¹ The need to progressively replace synthetic antioxidants is emphasized by their side effects, such as endocrine disruption or even carcinogenesis.¹² A large variety of polyphenolic compounds is found in *Vaccinium* species, that is why plants from this family, like *Vaccinium vitis-idaea* L. or *Vaccinium myrtillus* L, commonly known as lingonberry or bilberry, respectively, are intensively studied thanks to their significant antioxidant and antimicrobial activities.¹³ Wild bilberry (*Vaccinium myrtillus* L). is a spontaneous shrub found in mountain areas. Even though its fruits play an important role in diet, whether they are consumed as such, or processed, the leaves are also rich in polyphenolic compounds with potential biological activities, like antioxidant, antimicrobial, anti-inflammatory and antiproliferative activities, metabolic modulation, or skin health related activities.¹⁴⁻¹⁹

Interactions between polyphenols and proteins have been documented in the last decades since polyphenols have gained a lot of interest in the biomedical research area. Collagen mechanical and thermal properties can be enhanced through crosslinking, and polyphenols are among the agents that can fulfil this task (ie, tannic acid).²⁰ However, some

polyphenols could cause precipitation of proteins,²¹ thus in this study the polyphenolic bilberry leaves extract has been incorporated in functionalized mesoporous silica nanoparticles. Our group has previously reported the encapsulation of polyphenols from fruits and other medicinal plants in mesoporous silica supports for the enhancement of their stability over time.^{22–25} Since *V. myrtillus* fruits have been extensively studied compared to leaves, the valuable compounds from fruits have been more frequently the subject of encapsulation studies, especially in polysaccharides or vegetal protein matrices, in order to overcome the low stability of anthocyanins.^{26–30} To the best of our knowledge, the nanoconfinement of *V. myrtillus* leaves extract into mesoporous silica nanoparticles (MSN) was reported for the first time in this paper. There are only a few papers presenting the encapsulation of *V. myrtillus* leaves extract. Stefanescu et al used maltodextrin and glucose to encapsulate aqueous bilberry leaves extract by spray-drying method for an enhanced bioavailability of the polyphenolic compounds in the gastrointestinal tract.³¹ Kolisnyk et al formulated *V. myrtillus* leaves extract in sustained release tablets.³²

The mesoporous silica-type carriers used in this study were functionalized with organic groups that would enhance the affinity between MSN surface and collagen matrix, and at the same time to provide a favorable environment for the compounds of the polyphenolic extract. Thus, proline (a main component in the amino acids sequence in collagen) and propionic acid moieties were chosen since both can interact with collagen through hydrogen bonding and acid-base interactions.

Depending on their design, wound dressings can have a passive role, providing an optimal environment for healing, or they can be used as active wound dressings, enhancing the healing process and assisting in the possible complications that could occur. Herein we report the development of an active wound dressing, based on zinc-modified collagen porous scaffold, that would assist the wound healing process through the presence of zinc ions, and at the same time, bacterial infection would be prevented by the presence of the wild bilberry leaves extract. MSN were used in this study as a host for the polyphenolic extract to improve their stability over time and prevent the possible precipitation of the protein due to the presence of certain polyphenols from the wild bilberry leaves extract.

Materials and Methods

Materials

All reagents, solvents or enzymes were purchased from Sigma-Aldrich or TCI Chemicals and were used as received. (-)-Epigallocatechin gallate was purchased from Extrasynthese. The vegetal material, *Vaccinium myrtillus* or wild bilberry (WB) leaves, was collected from the natural habitat of Cindrel Mountains, Romania, at an approximate altitude of 1850 m. The plant material was identified and certified by the botanical specialist from National Institute for Chemical-Pharmaceutical Research & Development (INCDCF–ICCF Bucharest). The voucher specimen no. 3/2024 was stored in the Plant Material Room at INCDCF–ICCF Bucharest, Romania. The leaves were washed and dried in dark conditions, at room temperature. The dried leaves were used for the extraction of the phytochemicals after they were ground.

Wild Bilberry Leaves Extract Preparation

The wild bilberry polyphenolic extract (denoted WB) was prepared by ultrasound-assisted extraction using a plant: absolute ethanol ratio of 1: 10 (wt./vol). The vegetal material was soaked in ethanol overnight at room temperature, under constant stirring, and then heated at 50 °C under ultrasound irradiation for 1 h. The vegetal residue was filtered off and the solvent was removed under vacuum until constant mass was reached, and the extract was recovered as solid. The extract was redissolved in absolute ethanol at a certain concentration for further characterization.

Mesoporous Silica Nanoparticles Synthesis

Pristine MSN were synthesized according to the method previously reported.²³ Functionalization of pristine MSN was performed through post-synthesis procedure after applying high temperature treatment (550°C, 5 h) for the surfactant removal. Proline was linked to the surface of the MSN using (3-aminopropyl)triethoxysilane (APTES) through amide bonds formation by a newly developed approach. First, pristine MSN were impregnated with 20% (wt) proline (30 mg/mL aqueous solution). The suspension was shaken for 1 h on an orbital shaker (Grant bio-PSU-10i), and then water was

removed under vacuum, at room temperature, for another 12 h. Proline-impregnated MSN (100 mg) were dispersed in dry toluene (15 mL) and then the corresponding volume of APTES solution in toluene (120 mM) was added dropwise into the MSN suspension. The Pro: APTES molar ratio was 1:1. The reaction mixture was kept at reflux for 12 h, under constant magnetic stirring, followed by isolation of the solid through centrifugation and washing with acetone, ethanol and water. The sample, denoted MSN-Pro, was dried at room temperature. Carboxylic acid-modified MSN (MSN-COOH) were obtained through hydrolysis of cyanoethyl groups grafted on pristine MSN surface to propionic acid moieties, according to the method described elsewhere.³³

Wild Bilberry-Loaded MSN Carriers Preparation

The phytochemicals extracted from WB leaves were embedded through impregnation into the mesopores of functionalized MSN. After drying under vacuum (3 mbar) for 12 h, the mesoporous carriers were mixed with small volumes of ethanolic extract solution (10 mg/mL). After each corresponding volume was added, the mixture was homogenized, and ethanol was removed under vacuum. Then a following volume was added, and the process was repeated until an extract content of 25% (wt) was reached. Samples were denoted WB@MSN-Pro and WB@MSN-COOH.

Porous Scaffold Composites Preparation

Collagen was treated with 2% and 5% (wt) zinc ions to prepare the zinc-modified collagen scaffolds (CAR-Zn 2% and CAR-Zn 5%, respectively). Thus, 1 mL collagen acidic solution (1 mg/mL) was treated with the corresponding volume of zinc acetate (3.1 mM) aqueous solution at room temperature, for 2 h on an orbital shaker, at 250 rpm. The resulting solution was first frozen, and then freeze-dried at -80°C for 12 h using a Zirbus VaCo 2 freeze dryer.

The final composites were obtained by incorporation of the extract-loaded MSN into the collagen matrices. Thus, 42.5 mg extract-loaded mesoporous silica-type nanoparticles were suspended in 10 mL collagen and zinc-collagen solutions, respectively, and then aliquots were added to a 24 well plate. The plate was kept in a freezer for 12 h and then freeze-dried.

Polyphenolic Extract Characterization

Characterization of the wild bilberry extract was performed using spectrophotometric methods to determine total polyphenolic content (TPC) through Folin-Ciocalteu assay, total flavonoid content (TFC), total anthocyanins content (TAC) and radical scavenging activity (RSA) through DPPH and ABTS methods. The methods were previously described elsewhere.^{22,24} The half maximal inhibitory concentrations (IC_{50}) were determined for RSA of the extract through DPPH and ABTS assays, using linear regression for concentrations up to 850 $\mu\text{g/mL}$ (DPPH) or 550 $\mu\text{g/mL}$ (ABTS). Separation and identification of the polyphenolic extract components was performed on a Shimadzu Nexera X2 HPLC system with photodiode array detector, as previously described.²² Condensed tannins content (CTC) was assessed using the vanillin method.³⁴ Thus, to 50 μL sample (5 mg/mL concentration), 1.5 mL 4% vanillin methanolic solution and 0.75 mL 37% HCl were added. The reaction mixture was incubated at room temperature for 20 minutes and then the absorbance was measured at 500 nm. Triplicate experiments were conducted, and the results were expressed as catechin equivalents (CE).

Antidiabetic Activity via α -Glucosidase Inhibitory Assay

The α -glucosidase inhibitory activity was assessed using an adapted method proposed by Rupasinghe et al.³⁵ A mixture of 150 μL extract solution, 450 μL phosphate buffer solution (10 mM PBS pH 6.8) and 150 μL α -glucosidase from *Saccharomyces cerevisiae* solution (0.5 U/mL in PBS pH 6.8) were preincubated at 37°C for 15 min. Then, 150 μL *p*-nitrophenol- α -D-glucopyranoside (5 mM in PBS pH 6.8) were added and the reaction mixture was further incubated at 37°C for 15 min. The reaction was ended with 600 μL Na_2CO_3 (200 mM aq) and the sample absorbance was measured at 405 nm. α -Glucosidase inhibition activity was calculated with the following expression: $I (\%) = (1 - A_s/A_c) \cdot 100$, where $I (\%)$ represents percentage of inhibition, A_s and A_c represent the absorption of sample and control, respectively. For the control, PBS was used instead of extract solution, and this was considered 100% enzyme activity. At least five concentrations were tested in the linear domain for each sample. The enzyme inhibition percentage was plotted against

sample concentration and the results of α -glucosidase inhibitory activity were expressed as IC_{50} values, determined through linear regression for the ethanolic leaves extract, a commercial bilberry (CB) extract and (-)-epigallocatechin gallate (EGCG). Linear concentration domain for WB extract was 10–60 $\mu\text{g/mL}$ ($R^2 = 0.9926$), for CB extract 25–125 $\mu\text{g/mL}$ ($R^2 = 0.9983$) and for EGCG 1–20 $\mu\text{g/mL}$ ($R^2 = 0.9934$).

Characterization Methods

Small- and wide-angle XRD patterns were recorded on a Rigaku MiniFlex II diffractometer with Cu $K\alpha$ radiation ($\lambda=1.5418 \text{ \AA}$), in the range $1.2\text{--}6^\circ$, and $6\text{--}50^\circ$, respectively. FTIR spectroscopy was performed on a Bruker Tensor 27 spectrometer between 4000 and 400 cm^{-1} . Nitrogen adsorption/desorption isotherms were recorded on Micromeritics TriStar II Plus gas sorption analyzer, at 77 K. Pore size distribution (PSD) curves were computed with Density Functional Theory (DFT), specific surface area was determined through multi-point BET method, in the $0.02\text{--}0.25 P/P_0$ range, and total pore volume was determined at $P/P_0=0.99$. Differential scanning calorimetry (DSC) was recorded on a Mettler Toledo DSC 823e calorimeter, between 30°C and 200°C , under 80 mL/min nitrogen flow. Thermogravimetric analysis was carried out on a Netzsch STA 2500 Regulus in the $30\text{--}800^\circ\text{C}$ temperature range ($10^\circ\text{C}/\text{min}$), in synthetic air atmosphere. All spectrophotometric data were obtained on a Shimadzu UV-1800 spectrometer. SEM and TEM images were collected on a Tescan Vega 3 LMH microscope with an EDX detector and on a TECNAI G2 F30 S-TWIN microscope with a field emission gun, respectively.

Antimicrobial Activity Evaluation

Free and encapsulated extract was used against *P. aeruginosa* (ATCC 27853) and *S. aureus* (ATCC 25923) to assess the antimicrobial activity. The method was previously described using serial 2-fold dilutions method, in Mueller-Hinton broth,²³ in a 96 well plate. After incubation at 37°C for 24 h, the optical density was measured, and minimum inhibitory concentration (MIC) and minimum bactericidal concentration (MBC) were established. To demonstrate these values, after 6 h incubation of the bacterial strains with the tested samples, bacterial suspensions were collected from the wells and spread onto agar plates. The plates were incubated for 16 h and photographs were taken to demonstrate the inhibition of bacterial strains survival.^{36,37}

Cytocompatibility Assessment

Human normal keratinocytes HaCaT (ATCC - American Type Culture Collection, Manassas, VA, USA) were cultivated in RPMI 1640 medium with high glucose content supplemented with 10% fetal bovine serum (FBS) and 1% penicillin-streptomycin-neomycin antibiotic mixture (PSN) at 37°C and 5% CO_2 . For the cytocompatibility assay, different concentrations were tested. The assessment was performed after 24 h and 72 h incubation by MTT assay, as previously described.³⁸

Anti-Inflammatory Potential Evaluation

The anti-inflammatory potential of the encapsulated bilberry extracts was performed on HaCaT keratinocytes. Briefly, HaCaT cells (1×10^6 cells/mL) cultivated in RPMI 1640 medium, supplemented with 10% FBS and 1% PSN antibiotic mixture, were stimulated by incubation with 10 ng/mL LPS (lipopolysaccharide). Further, they were exposed for 18 h to different concentrations of free and encapsulated bilberry extracts. The culture media were collected, centrifuged for 10 min at $400 \times g$, and their content was analyzed for the IL- 1β and TNF- α cytokines using ELISA kits.

Cytotoxicity Assessment

Human skin carcinoma MelJuso cells (ATCC - American Type Culture Collection, Manassas, VA, USA) were cultivated in RPMI supplemented with 10% FBS and 1% PSN antibiotic mixture at 37°C and 5% CO_2 . The cytotoxic potential was determined through MTT test, at the same time intervals, after MelJuso cells were seeded and treated in the same conditions as HaCaT keratinocytes.

Apoptotic Effect Evaluation

The apoptosis of MelJuso cells induced by the encapsulated bilberry extracts was assessed as previously described.²³ Briefly, MelJuso cells were stained with Dead Cell Apoptosis Kit and analyzed on an LSR II BD flow cytometer (Becton Dickinson).

Wound Healing Potential Evaluation

The wound healing potential of the scaffolds was evaluated by scratch assay. Fibroblast cells (NCTC cell line) were seeded in 24 well plates (1×10^5 cells/well) and cultivated in DMEM growth medium, supplemented with 10% FBS and 1% PSN antibiotic mixture, at 37°C. After 24 h cultivation of a cellular monolayer, the simulated wound scratch was obtained as a perpendicular linear scratch. Cellular debris was removed after careful washing with PBS and the porous scaffolds were added. Cells were maintained with the porous scaffolds at 37°C for 24 h. The analysis of the migration potential was monitored with an inverted microscope (Axio Star Plus) immediately after the scratch ($t = 0$) and after 19 h ($t = 19$ h), to evaluate the closure of the simulated wound.

Statistical Analysis

Experimental results are presented as mean value \pm standard deviation ($n=3$). Statistical differences were analyzed using Student's *t*-test, two-tailed, two-sample equal variance on each pair of experimental data using Microsoft Office 365 Excel software. For $p < 0.05$, significant statistical difference was considered.

Results and Discussion

Properties of Wild Bilberry Leaves Extract

The composition of the ethanolic extract was assessed through HPLC-PDA analysis and the components are presented in Table 1. Six compounds were identified in the extract: chlorogenic acid, rutin hydrate, epicatechin and catechin hydrate, and also *p*-coumaric acid and *trans*-ferulic acid in lower quantities. Chlorogenic acid was found in the highest concentration among the polyphenols identified in the bilberry leaves extract. This was also confirmed by previous studies that have used bilberry leaves with different origin, various extraction methods or solvents.^{13,31,39,40} High concentrations of rutin and epicatechin have also been detected in the WB ethanolic extract. Other studies have not reported such high concentration of epicatechin, probably due to its low water solubility and the use of water or aqueous solvent mixtures as solvent extraction.^{13,31,39,41}

The radical scavenging activity and quantitative estimation of total polyphenols (TPC), total flavonoids (TFC), condensed tannins (CTC), and total anthocyanins (TAC) in the wild bilberry leaves extract (WB) were evaluated by colorimetric methods and the values were presented in Table 2 with respect to the dry extract mass. TPC (24.91 ± 0.38 mg GAE/g plant) was higher than that of previously reported bilberry leaf extracts obtained by ultrasound-assisted extraction (196.48 – 259.70 mg GAE/g dry extract),²⁴ microwave assisted extraction (118.7 – 166.1 mg GAE/g dry extract)⁴² or other conventional methods, like Soxhlet or maceration (173.19 and 217.59 mg GAE/g dry extract, respectively).³⁹ TFC was expressed as quercetin and rutin hydrate equivalents (QE and RHE) since the two flavonoids have different chemical structures and could generate false-positive or negative contributions to the TFC depending on the composition of the extract.⁴³ TFC expressed as RHE was three times higher (8.94 ± 0.01 mg RHE/g plant) than that expressed as QE (2.98 ± 0.01 mg QE/g plant). These results might be an indication that the extract is richer in flavonoid glycosides than flavonoids, which could be correlated with the high concentration of rutin hydrate found in the leaves extract, while quercetin was not identified at all. This is supported by the work of Bujor et al⁴² and Tian et al.¹⁹ They

Table 1 Composition of WB Leaves Ethanolic Extract

Concentration (mg / g extract)					
Catechin hydrate	Chlorogenic acid	Epicatechin	<i>p</i> -Coumaric acid	<i>trans</i> -Ferulic acid	Rutin hydrate
7.396 \pm 0.030	81.028 \pm 0.003	26.365 \pm 0.060	0.310 \pm 0.001	0.095 \pm 0.002	31.214 \pm 0.010

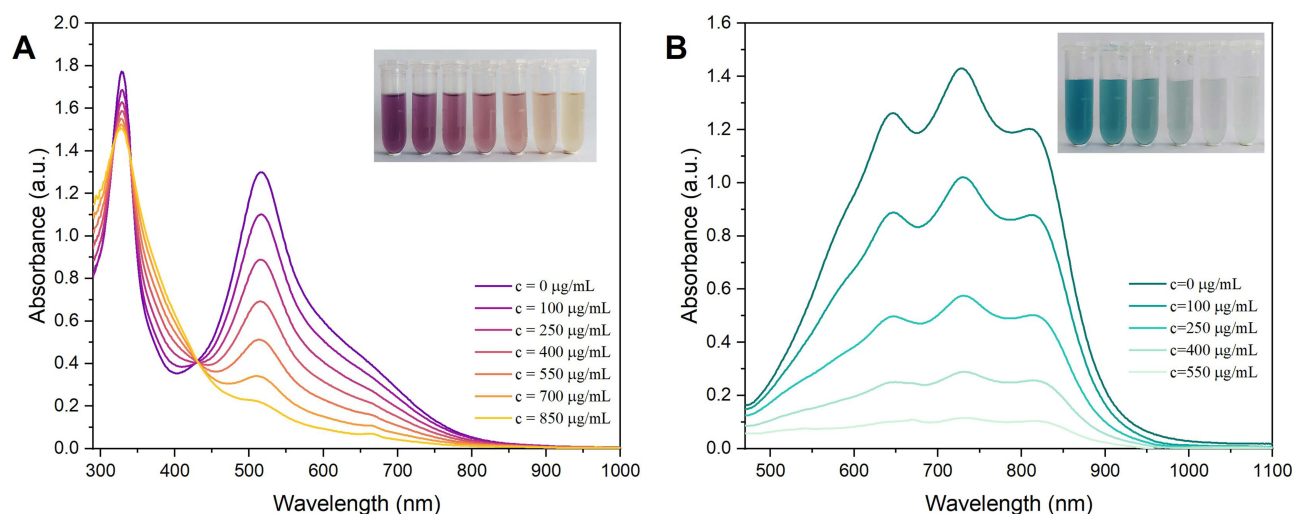
Table 2 Properties of WB Leaves Extract with Respect to Dry Extract Mass

TPC mg _{GAE} / g _e	TFC mg _{flavonoid} / g _e	TAC mg _{CGE} / g _e	CTC mg _{CE} / g _e	DPPH		ABTS	
				IC ₅₀ μg _e / mL	RSA mg _{TE} / g _e	IC ₅₀ μg _e / mL	RSA mg _{TE} / g _e
336.58 ± 5.11	40.25 ± 0.15 (QE) 120.83 ± 0.14 (RHE)	4.84 ± 0.47	146.66 ± 2.50	455.63 ± 12.21	700.61 ± 5.09	269.37 ± 18.91	283.26 ± 5.70

Abbreviations: TPC, total polyphenolic content [mg_{Galic Acid Equivalents}/g_{extract}]; TFC, total flavonoids content [mg_{Quercetin/Rutin Hydrate Equivalents}/g_{extract}]; TAC, total anthocyanins content [mg_{Cyanidin-3-Glucoside}/g_{extract}]; CTC, condensed tannins content [mg_{Catechin Equivalents}/g_{extract}]; IC₅₀, half maximal inhibitory concentration of DPPH and ABTS [μg_{extract}/mL]; RSA, Radical Scavenging Activity [mg_{Trolox Equivalents}/g_{extract}].

obtained a higher concentration of flavonol glycosides compared to flavonol monomers in bilberry leaves extracts. Bilberry fruits are rich in anthocyanins, but low anthocyanins concentration was found in the leaves as well (0.358 ± 035 mg_{CGE}/g_{plant}), similar to those published by Stefanescu et al.¹³ Condensed tannins, also known as proanthocyanidins, are phenolic oligomers or polymers, where catechin or epicatechin are the most representative monomeric units. CTC value assessed by vanillin-HCl assay was 10.85 ± 0.19 mg_{CE}/g_{plant}. The antioxidant activity of WB leaves extract was assessed through DPPH and ABTS assays and expressed as Trolox equivalents (TE). RSA values were 51.85 ± 0.38 mg_{TE}/g_{plant} for DPPH assay and 20.96 ± 0.42 mg_{TE}/g_{plant} for ABTS. In terms of RSA, the WB extract was better than previously reported ethanolic extracts, however hydroethanolic extracts proved to have higher RSA.²⁴ Various concentrations of extract solution were added to the ABTS and DPPH solution in order to evaluate the concentration of extract that inhibits 50% of radicals in the solution (Figure 1). The IC₅₀ values were determined from the linear regression of radical scavenging activity (%) against extract concentration (μg/mL). The equations resulted were RSA (%) = 0.1098 * c(μg/mL), R²=0.9964 for DPPH, and RSA (%) = 0.1862 * c(μg/mL), R²=, 0.9808 for ABTS. The corresponding IC₅₀ values determined from these equations were 455.63 ± 12.21 μg/mL and 269.37 ± 18.91 μg/mL, respectively. The IC₅₀ values were different for DPPH and ABTS, with higher value obtained for DPPH. The differences come from the structural differences of the two radicals and from the radical scavenging assays, since ABTS is more compatible with hydrophilic compounds, and DPPH is more suitable for hydrophobic compounds.

Bilberry leaves are rich in catechins and their derivatives, which are known for their antidiabetic properties. Catechins and their gallate derivatives interfere with α-glucosidase activity, by preventing digestion of carbohydrates, thus improving blood glucose levels.⁴⁴ The inhibitory activity of the extract against α-glucosidase was evaluated by determining IC₅₀. IC₅₀ value for WB extract, 35.81 ± 2.51 μg/mL, was similar to that reported for bilberry leaves aqueous extract (30.46 ± 0.98 μg/mL) by Takacs et al,⁴⁵ and lower than those obtained by Bljajic et al for aqueous (2.53

**Figure 1** Radical scavenging activity of wild bilberry leaves extract assessed through DPPH (A) and ABTS (B) at various concentrations.

± 0.21 mg/mL) and hydroethanolic extracts (0.29 ± 0.02 mg/mL).⁴⁶ In this study, the WB extract was compared with a commercially available *V. myrtillus* extract prepared by maceration in water-glycerin-ethanol mixture. This commercial extract showed a lower α -glucosidase inhibitory activity (95.94 ± 3.29 μ g/mL), demonstrated by the higher IC_{50} value compared to that of WB extract. (-)-Epigallocatechin gallate (EGCG) was used as positive control for α -glucosidase inhibitory activity. The IC_{50} obtained for EGCG is the equivalent of 20.13 ± 1.33 μ M (9.23 ± 0.61 μ g/mL). Similar results were obtained by Xu et al and Li et al^{47,48} Other studies mentioned slightly higher values of IC_{50} for EGCG,^{49,50} however in all cases EGCG proved a three to five times better inhibition of α -glucosidase compared to acarbose, which is a standard prescribed anti-diabetic drug that inhibits α -glucosidase activity. Even though catechin derivatives are known for their inhibition of α -glucosidase, other polyphenols, like chlorogenic acid or rutin, also show inhibitory activity of α -glucosidase,^{51,52} so these might contribute to the antidiabetic activity of the prepared WB extract as well.

Physicochemical Characterization of Mesoporous Carriers and Extract-Loaded Carriers

The amino acid-functionalized MSN were obtained through a new method proposed in this paper. Other methods reported for amino acid modification of MSN include reactions between an amino acid and chloropropyl-,⁵³ glycidyloxypropyl-,⁵⁴ or amine-functionalized MSN. For the last type of reaction usually an activation agent for –COOH group of the amino acid is used, like carbodiimides,⁵⁵ uronium salts,⁵⁶ or imido-phosphonium salts.⁵⁷ The method proposed in this paper is simple, effective and does not require an activating reagent. The functionalization of the mesoporous materials was evidenced through FTIR spectroscopy and TGA analysis. The structural features of functionalized MSN were assessed by small-angle XRD, the textural properties were evaluated by N₂ adsorption/desorption isotherms, and the morphological features were illustrated by SEM and TEM microscopy.

The new method proposed for the functionalization of MSN-Pro proved to be successful. The FTIR spectrum (Figure 2A) confirmed the presence of the amide II specific vibration band. This band was observed at 1546 cm^{-1} and was ascribed to N–H deformation vibration coupled with C–N stretching vibration characteristic for amides.⁵⁸ The amide I band, assigned to C=O vibration in the amide bond, is usually present at 1650 cm^{-1} .⁵⁸ This band cannot be distinguished in the FTIR spectrum of MSN-Pro sample because it overlaps the band at 1630 cm^{-1} , which is attributed to physio-adsorbed water molecules on the silica surface. The C=O stretching vibration of MSN-COOH was identified at 1716 cm^{-1} (Figure 2A).

As seen in the SEM (Figure 2B) and TEM (Figure 2C) images, silica nanoparticles were predominantly spherical, with an average size of 137 ± 10 nm, but slightly ellipsoidal nanoparticles could also be observed with a width: length ratio of 1: 1.2–1.4. The structural characteristics of MSN were evidenced in the small-angle XRD patterns (Figure S1) and discussed in Supplementary Material. The partially disordered pore array of the pristine silica nanoparticles was confirmed by TEM image (Figure 2C), where a radial distribution of cylindrical and worm-like mesopores was depicted, showing a short-range ordering of the mesopores.

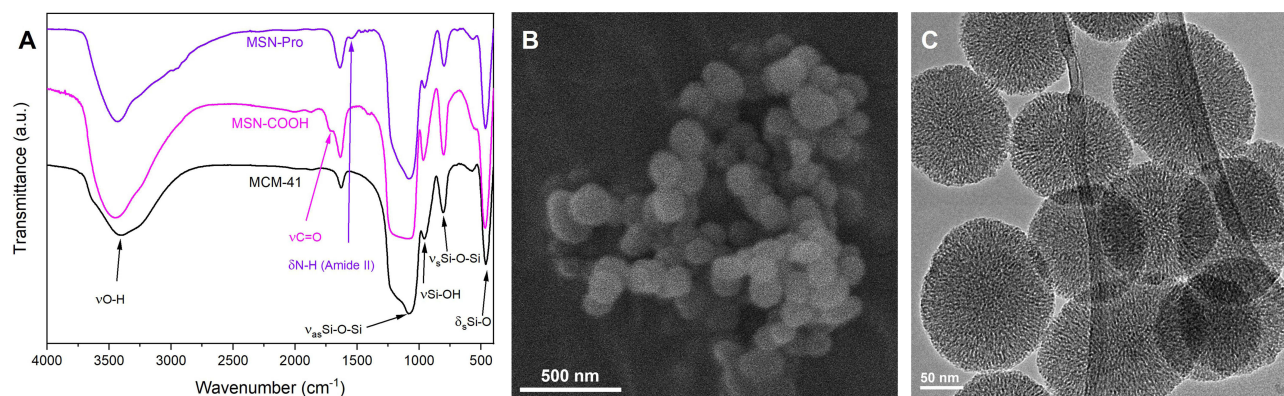


Figure 2 (A) FTIR spectra of pristine and functionalized MSN carriers; (B) SEM image of MSN-Pro; (C) TEM image of pristine MSN.

Table 3 Textural Properties of MSN Carriers

MSN carrier	d_{DFT} (nm)	S_{BET} (m ² /g)	$V_{p < 10 \text{ nm}}$ (cm ³ /g)	SiO ₂ :FG molar ratio
MSN	4.41	889	0.775	–
MSN-Pro	3.81	790	0.609	1:0.063
MSN-COOH	4.25	632	0.478	1:0.044

Abbreviations: d_{DFT} , average pore diameter calculated with NLDFT method; S_{BET} , specific surface area computed with BET model; $V_{p < 10 \text{ nm}}$, pore volume for pores with diameter smaller than 10 nm; FG, functional group.

The mesoporous nature of the silica nanocarriers was confirmed by the type IV N₂ adsorption/desorption isotherms (Figure S2). After functionalization of the pristine nanoparticles, average pore size decreased from 4.41 nm to 4.25 nm and 3.81 nm for MSN-COOH and MSN-Pro, respectively (Table 3). The decrease of the average pore size is correlated with the size of the functional group attached to the silica pore walls through post-synthesis procedure, as N-propylpyrrolidine-2-carboxamide group is larger than propanoic acid moiety. The hydrolysis of cyanide group to carboxylic acid caused a partial collapse of the mesoporous structure, which decreased the specific surface area (S_{BET}) and pore volume ($V_{p < 10 \text{ nm}}$) of the MSN-COOH carrier more than the introduction of a voluminous functional group, as is the case of MSN-Pro (Table 3). The results obtained from N₂ adsorption/desorption isotherms of MSN-COOH were in agreement with the XRD pattern, which showed a less intense main diffraction peak. The S_{BET} and $V_{p < 10 \text{ nm}}$ values of the functionalized MSN decreased in comparison with those of pristine MSN (Table 3). Even though a decrease of the porosity data was registered after the introduction of organic groups, the functionalized carriers have adequate porosity that would enable them to be used as carriers for cargo molecules. The organics decomposition was evaluated from TGA analysis (Figure S3), and it was accounted as the content of functional groups (FG), which was expressed as molar ratio towards SiO₂ in Table 3.

Polyphenols tend to have a lower stability in time, due to environmental factors, such as light, high temperature, or humidity.^{24,59,60} Previous reports showed that the immobilization of polyphenolic extracts into mesopores of silica carriers led to enhanced stability over time.^{22–24} After MSN-Pro and MSN-COOH carriers were loaded with polyphenolic extract through impregnation followed by solvent removal, the exact amount from the mesoporous carriers was evaluated by TGA (Figure S3) up to 650°C. The extract content was 23.5% for MSN-Pro and 27.2% for MSN-COOH. SEM investigation of WB@MSN-Pro showed no extract molecules on the carriers surface (Figure S4A).

After six-month of storage at 4°C the radical scavenging activity (RSA) of the encapsulated extract was also evaluated through DPPH assay and compared to that of the extract. The RSA values of the encapsulated extracts are similar to that of the extract alone (Figure S4B), thus suggesting a good stability of the extract over time, which is preserved through incorporation of the polyphenolic compounds into the mesopores. The carriers were also tested, and compared to the DPPH solution, which was used as control. MSN-COOH support presented similar RSA to the control, however MSN-Pro showed a slight increase in RSA value, due to possible interference between DPPH and the functional groups of the carrier.

In vitro Biological Activities of Wild Bilberry-Loaded MSN Carriers

In vitro antimicrobial activity, biocompatibility, anti-inflammatory activity, antiproliferative activity and apoptotic effect on cancer cells of extract-loaded samples were assessed. The tested extract showed good biocompatibility at concentrations up to 50 µg/mL, illustrated by the high values of normal human keratinocytes viability after 24 h (Figure 3A). After 72 h, the cell viability in the group treated with encapsulated WB extract was similar to that registered for the free extract. Concentrations of embedded extract, up to 50 µg/mL, proved to not interfere significantly with cellular proliferation. The percentage of viable cells varied between 100% and 81.61%, after 24 h, which indicates a good biocompatibility of the incorporated extract samples on keratinocytes.

Inflammation is essential for several defense mechanisms, and it is crucial in the context of the growing number of chronic diseases based on inflammatory processes. Development of potent and, even more important, of natural derived

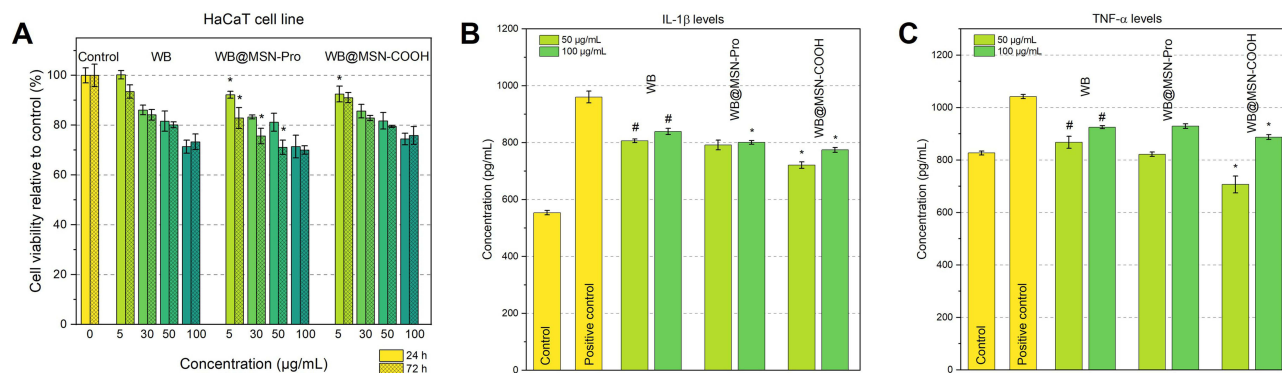


Figure 3 (A) Cytocompatibility of *Vaccinium myrtillus* extract and encapsulated extracts in human keratinocytes normal cells after 24 and 72 h incubation; Secretion of IL-1 β (B) and TNF- α (C) pro-inflammatory cytokine in pretreated HaCaT cells with different concentrations of bilberry extracts, determined by ELISA assay at 24 h cultivation. # $p < 0.05$ compared to positive control; * $p < 0.05$ compared to WB.

inhibitors for inflammation mediators represents a high priority in the pharmaceutical field. The obtained results indicate the anti-inflammatory potential of all tested samples, with reduced levels of IL-1 β (Figure 3B) and TNF- α (Figure 3C) cytokines when compared to the positive control (treated with LPS). The strongest anti-inflammatory activity was registered for WB@MSN-COOH treatment, for which levels of IL-1 β (721.33 pg/mL) and TNF- α (706.94 pg/mL), for 50 $\mu\text{g}/\text{mL}$ concentration, were lower than the positive control, that registered 960.45 pg/mL IL-1 β and 1041.94 pg/mL TNF- α , respectively. The trend was maintained for the highest concentration tested, 100 $\mu\text{g}/\text{mL}$, where WB@MSN-COOH was the most efficient, followed by WB@MSN-Pro and WB extract alone (Figure 3B and C). The anti-inflammatory potential is highly relevant in the context of inflammation as a key player in the pathogenesis of different chronic diseases. There are studies showing the anti-inflammatory effects of bilberry fruit extracts in in vivo studies, such as inhibition of ear oedema and liver inflammation along with a consistent suppression of increased levels of iNOS, TNF- α , IL-1 β and IL-6⁶¹ or reduction of neurological inflammation offering a protective effect against microglial cells death.¹⁸

Antibacterial activity of the bilberry extract, alone and entrapped into mesoporous carriers, was assessed against *P. aeruginosa* and *S. aureus* bacterial strains. The MIC and MBC were determined after measuring the optical density of the suspensions. These results were further confirmed after incubation of the suspensions on agar plates (Figure 4). In the case of MBC, the concentrations of tested samples inhibited completely the microorganisms growth, while in the case MIC, bacterial strains are still visible, however, there is a lower survival rate compared to the corresponding control. The encapsulated extract showed stronger antimicrobial activity, demonstrated by the lower concentrations that interfered with bacterial proliferation. The lowest MIC (3.9 mg/mL) was registered for WB@MSN-Pro on both strains, while the lowest MBC obtained for the same sample was 7.81 mg/mL. The tested samples were more effective against *S. aureus*. The results were in agreement with those obtained by Tian et al, that demonstrated high inhibitory effects of bilberry fruit and leaf extracts towards *S. aureus*, *L. monocytogenes* and *B. cereus*.¹⁹ The WB extract prepared for this study showed better MIC (15.62 mg/mL) and MBC (31.25 mg/mL) values against *P. aeruginosa* strain than the hydroethanolic one reported by Gil-Martinez et al, but lower antibacterial activity against *S. aureus* strain.⁴⁰ Our WB extract showed MIC = 7.81 mg/mL and MBC=15.62 mg/mL on *S. aureus* strain. Several mechanisms of action were suggested for polyphenols antibacterial activity, such as disruption or permeabilization of cells membrane, or direct effects on microbial metabolism.⁶² The results obtained contributed to the perspective of using polyphenols as antibacterial agents, and the entrapment of WB extract showed an enhanced antibacterial activity against Gram-positive and Gram-negative bacterial strains.

In parallel with biocompatibility, the antiproliferative effect of *Vaccinium myrtillus* extract encapsulated in mesoporous silica-type matrices was also investigated on MelJuso cancer cells. After 72 h treatment, the encapsulated extract significantly decreased cells viability compared to the extract alone, starting with 50 $\mu\text{g}/\text{mL}$ concentration (Figure S5A). Chlorogenic acid, the major constituent in the WB leaves extract, was shown to not influence the proliferation of human tumor HeLa cells, however it exhibited cancer-preventive activity.⁶³ The antiproliferative activity of the WB bilberry

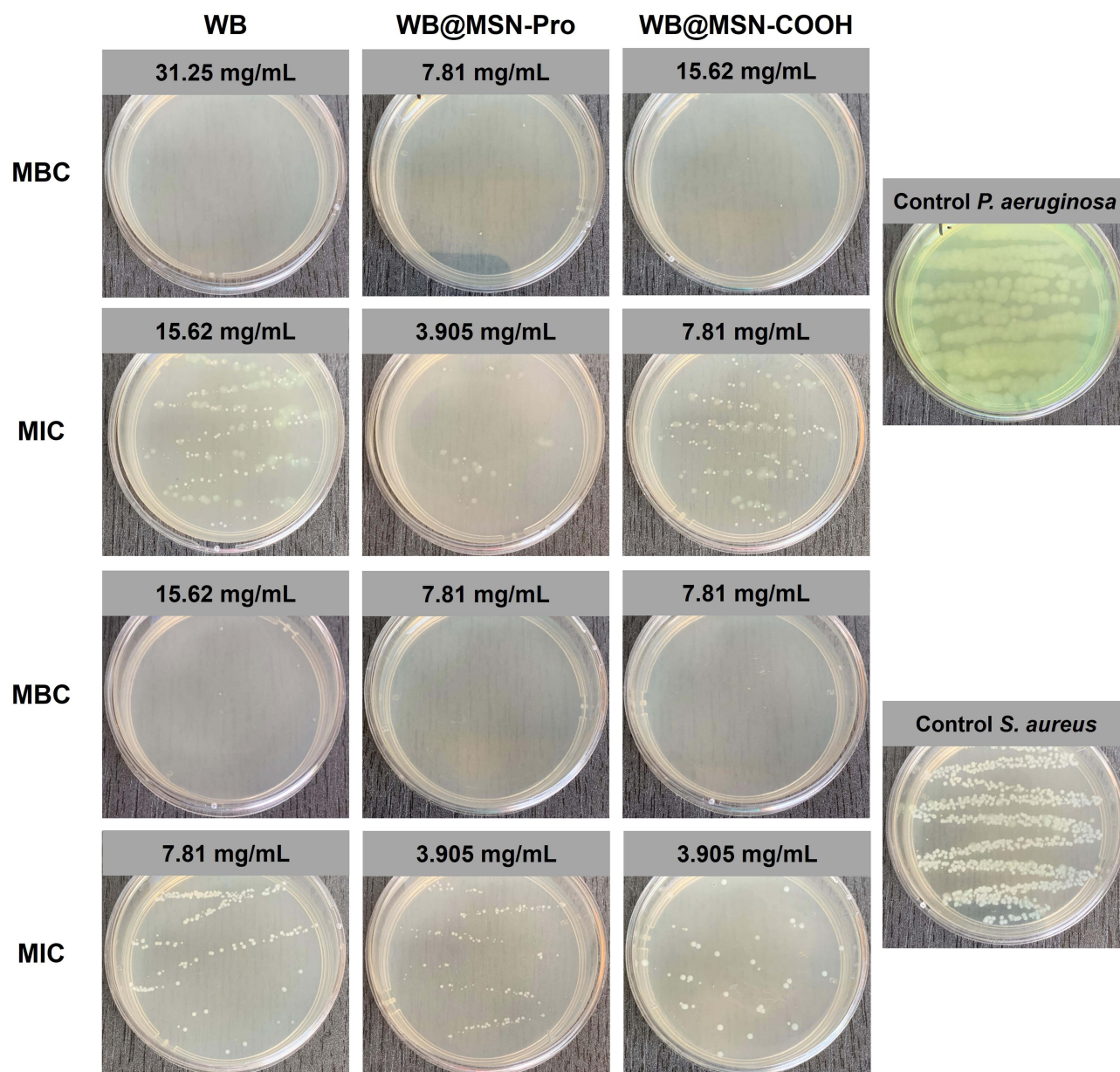


Figure 4 *P. aeruginosa* and *S. aureus* bacterial strains survival at MBC and MIC of tested samples.

extract on MelJuso cells is most likely owed to the synergistic activity of the extract components. For concentrations where low MelJuso cell viability was recorded (MTT test), higher number of apoptotic cells was noticed in the early stage of apoptosis for the free and incorporated extract samples (Figure S5B).

Numerous compounds from vegetal sources have shown antioxidative and antiproliferative properties in in vitro tests. The antiproliferative potential of bilberry leaf extracts was shown on various colorectal cancer cells, such as HT-29, T-84, SW-837⁴⁰ and gastric cancer cells, like AGS,⁶⁴ generally higher concentrations and longer exposure times leading to a better cell proliferation inhibition. An important limitation when comparing studies is the inconsistency due to the different chemical compositions of the tested extracts. Equally important are the differences based on season or location of plants on variations of polyphenolic components in leaves, stems and fruits and their associated biological activities.^{13,39,41,42}

Physicochemical Properties of Zinc-Modified Collagen Porous Scaffold

Zinc-modified collagen porous scaffolds morphology was assessed by SEM, and EDX mapping was used for the evaluation of zinc distribution. The physicochemical properties were evaluated by FTIR spectroscopy and DSC analysis, and structural features were evidenced in the wide-angle XRD patterns.

Besides terrestrial mammals, marine organisms are also a valuable source of collagen, and very little explored, even though it would be a sustainable extraction method from fish processing industry waste or from harvesting invasive species. Collagen used in this study comes from a marine gastropod mollusk, *Rapana venosa*, and has been previously described.³⁸ Zinc acetate was chosen as zinc source for the development of the zinc-modified collagen porous scaffold that would serve as host for the antimicrobial composites. Zinc acetate is used in cosmetic formulations as astringent or biocide,⁶⁵ and it is approved as active ingredient in over the counter (OTC) medications for skin protection.⁶⁶ Furthermore, a compatibility between the counterions of zinc salt and acetic acid used for the collagen solubilization was intended. Zinc salts were tested on animals for dermal irritation and zinc acetate produced skin irritation at concentration of 20% (wt), while zinc chloride or sulphate were irritating at 1% (wt) concentrations.⁶⁷ In this study, two zinc concentrations were considered 2% and 5% (wt) with respect to collagen.

The collagen porous scaffold (Figure S6) is formed by smooth layers of collagen sheets, with disordered pores distribution and irregular sizes. The morphology of the porous scaffolds was retained after zinc introduction into the matrix, regardless of the zinc content. Uniform distribution of zinc, illustrated in red in Figure 5A and B, was detected through EDX mapping for

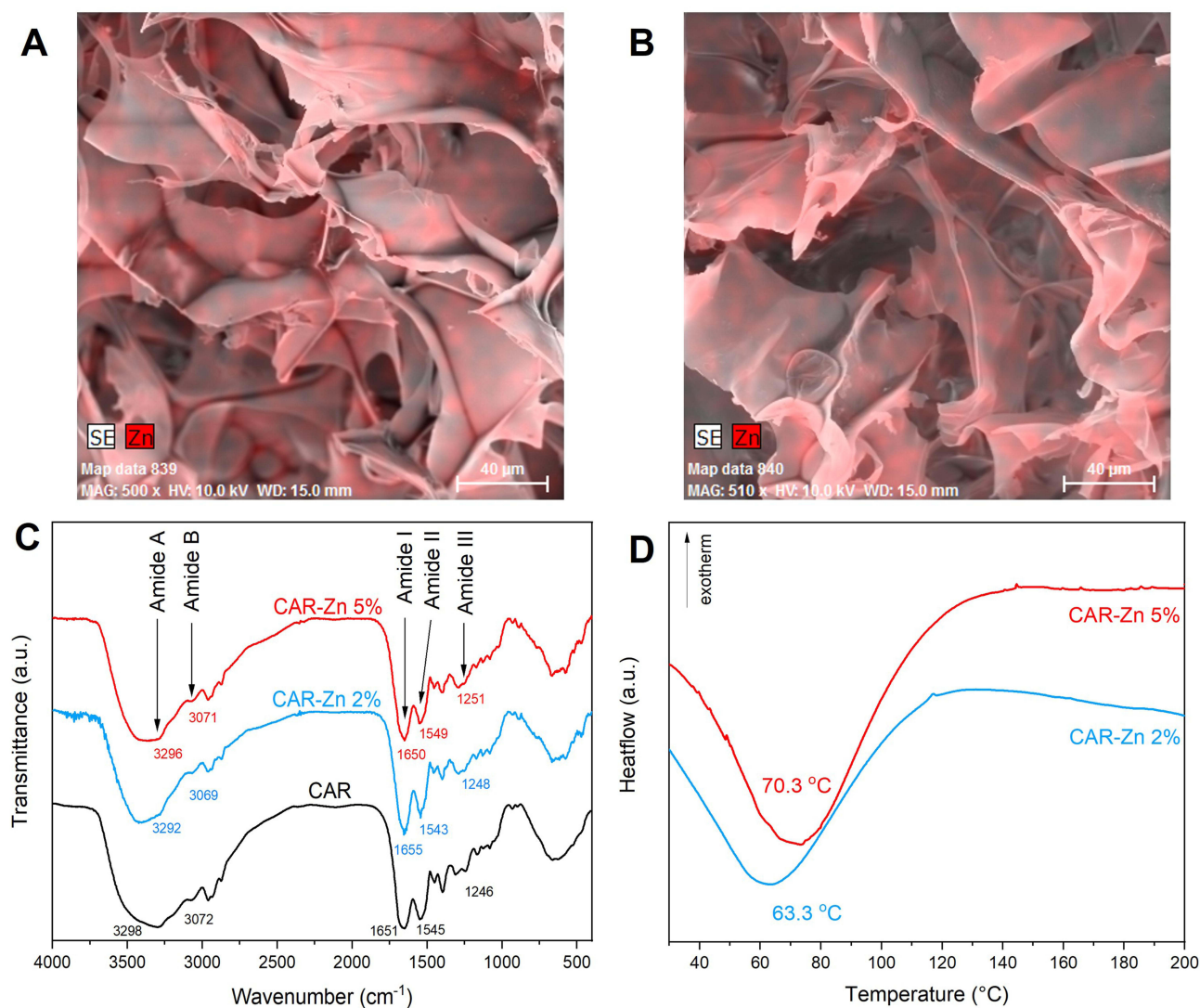


Figure 5 SEM images with EDX mapping of CAR-Zn 2% (A) and CAR-Zn 5% (B) into collagen matrix; (C) FTIR spectra of zinc-modified collagen porous scaffolds; (D) DSC analysis of CAR-Zn 2% and CAR-Zn 5%.

both samples with 2% and 5% zinc content. No zinc acetate crystals were noticed into the porous scaffold; therefore, we can consider that protein chelated all zinc ions.

One of the main problems in working with protein matrices is their denaturation, with respect to their thermal and structural stability. Our previous study has shown a preservation of the α -helix chains of collagen after functionalized MSN were included into the protein matrix.²³ In this study, zinc was used for its anti-inflammatory properties when used in topical applications.¹⁰ Supplementary zinc in wound dressings stimulated keratinocytes mobility, thus improving the wound healing process.⁶⁸ Previous reports of collagen-zinc complexes indicated a maximum 9% content of zinc ions chelated by bovine collagen,⁶⁹ while Meng et al reported the equivalent of 32.2% Zn^{2+} chelated by peptides from fish skin.⁷⁰

Proteins are susceptible to degradation induced by environmental conditions and/or interactions with other molecules, therefore the evaluation of secondary structure of proteins is a very useful tool in the assessment of their denaturation.⁷¹ The secondary structure of proteins is established by the position of the amide I and II bands in the FTIR spectra, so the structure of collagen porous scaffold modified with zinc was assessed through FTIR spectroscopy. The position of amide I at $\sim 1650\text{ cm}^{-1}$, given by the C=O stretching vibration coupled with N-H bending and C-N stretching vibrations, demonstrated the α -helical structure of the pristine protein, and the same was revealed for the other two zinc-modified protein matrices. Compared to pristine collagen scaffold, there were only minor shifts of the main amide bands for the scaffolds with 2% and 5% Zn^{2+} , illustrated in [Figure 5C](#). The positions of the bands suggest a preservation of the protein structure for both selected zinc concentrations. These results are in agreement with previous reports that showed that introduction of transition metal ions, like Cu^{2+} or Zn^{2+} , in low concentration (0.4 mM~2% towards collagen) did not affect the secondary structure of collagen.⁵

The other issue concerning proteins is related to their thermal stability. The thermal behavior of zinc-modified collagen matrices was assessed through DSC analysis. The presence of Zn^{2+} ions had an important influence on the denaturation temperature (T_d) of the porous scaffolds. In our previous study, we reported a T_d of 57°C for pristine collagen.²³ The results in this work showed an increased denaturation temperature of the collagen scaffold due to the complexation of zinc ions with the protein ([Figure 5D](#)). Furthermore, an increasing denaturation temperature was registered with increasing zinc content, thus for 2% Zn^{2+} content $T_d = 63.3^\circ\text{C}$ and for 5% Zn^{2+} content $T_d = 70.3^\circ\text{C}$. Denaturation temperature is important in biological applications since the properties of the composite should be preserved at body temperature and CAR-Zn 5% showed the highest thermal stability, without causing denaturation on the protein conformation.

Structural information of the collagen porous scaffold was also obtained from X-ray diffraction ([Figure S7](#)). The collagen scaffolds usually show a diffraction peak, at $2\theta \sim 9^\circ$,⁷² which illustrates the intermolecular lateral packing of collagen. There was a small shift of the diffraction peak towards higher 2θ values, which indicated lower d spacing values in zinc-modified collagen diffraction pattern ($d_I = 9.29\text{ \AA}$) compared to pristine collagen ($d_I = 9.64\text{ \AA}$). This means that there is a reduction of the intermolecular lateral packing of collagen, which is another proof that the amino acids on the side chains chelated the zinc ions.

Assessment of Wound Healing Potential of Composites

For the development of the final composites, the bilberry extract embedded into MSN-Pro carrier (WB@MSN-Pro), that showed the best antimicrobial potential on both Gram-positive and Gram-negative bacterial strains, was included into the collagen matrix modified with 5% zinc, which proved good structural and thermal stability. Preliminary steps into developing the composites based on zinc-collagen scaffolds included testing of a hydroethanolic bilberry leaves extract, however the interactions between this extract and solubilized collagen caused protein precipitation. The explanation could be that water soluble components irreversibly interacted with collagen and led to its denaturation. This is supported by literature reports showing that tannins form insoluble products with proteins via hydrogen bonding.⁷³ The results in our study, show that WB extract contains condensed tannins ([Table 2](#)), however they do not affect the collagen conformation, which might suggest that tannins extracted in aqueous medium or other water-soluble compounds are responsible for this denaturation.

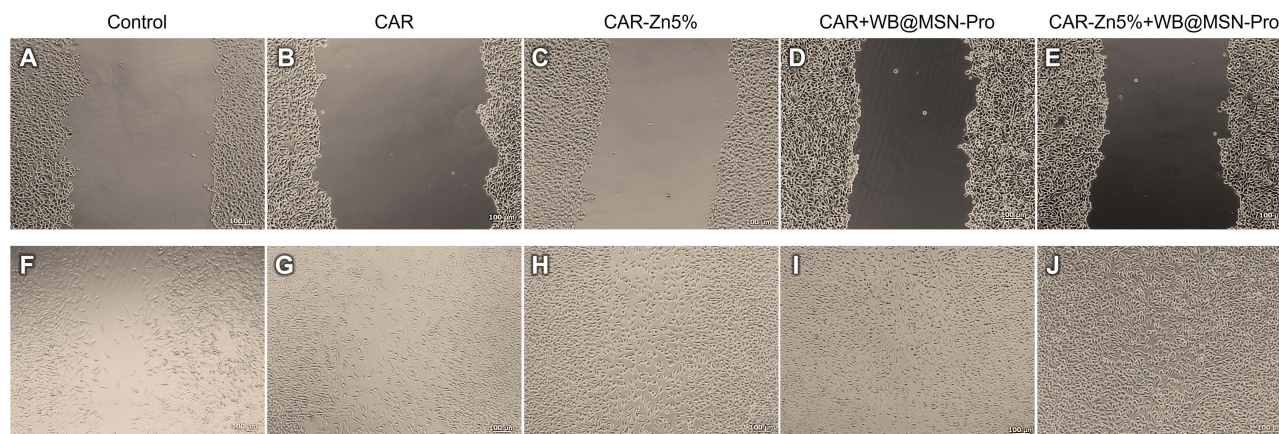


Figure 6 Optical micrographs of cell migration processes, comparative study, time $t = 0$ (A–E) versus $t = 19$ h (F–J). Scale bar 100 μ m.

The final step of the current research study was to evaluate the possibility of using the novel composites comprising of zinc-modified collagen and wild bilberry leaves extract embedded in MSN-Pro in skin wound healing. The wound healing capacity of the designed composites was assessed through the scratch assay. This method consists of performing a linear scratch on cells arranged in a single layer and evaluating cells migration after the scratch.⁷⁴ Fibroblasts are found in the lower layer of the skin, the dermis, so the wound healing potential of the composites was assessed on a fibroblast cell line. Optical microscope images were collected immediately after the scratch (Figure 6A–E) and after 19 h exposure to the tested samples (Figure 6F–J). The images revealed that the fibroblast migration was enhanced in the presence of the tested scaffolds. It is worth noting that a natural tendency of the fibroblast cells to migrate was observed also for control, untreated cells culture (Figure 6F). The influence of zinc presence was evaluated on NCTC fibroblasts mobility and compared to pristine collagen porous scaffold. Besides repairing tissues, cells migration has an important role in immunity and tissue homeostasis. In this study, an enhanced cells migration was observed in the presence of collagen scaffolds (Figure 6G), especially for the zinc-modified one (Figure 6H). Our results are in agreement with previous reports, which showed that the presence of zinc in hydrogel dressings enhanced migration of HFS fibroblasts and HaCaT keratinocytes⁷⁵ and chondroitin sulphate modified with zinc accelerated wound healing in in vivo experiments.⁷⁶ Considerable differences were observed for the collagen scaffolds with vegetal extract (Figure 6I and J) in comparison with pristine collagen scaffold (Figure 6G), which indicated a positive effect of the WB leaves extract on the mobility of the fibroblasts. Complete closure of the scratch was detected for the scaffolds loaded with encapsulated WB extract and zinc (Figure 6J). Similar results were reported by Vedhanayagam et al that highlighted both the in vitro (keratinocytes) and in vivo (Wistar Albino rats) wound healing potential of collagen-based scaffold containing spherical ZnO nanoparticles.⁷⁷

Conclusion

These results can contribute to the increasing interest for wound-healing solutions. Based on the stability of zinc-modified collagen porous scaffold, we can conclude that the introduction of zinc ions in concentrations of up to 5% into the collagen matrix does not affect the secondary structure of the protein, as FTIR spectroscopy confirmed, and the stability of the protein is enhanced, as DSC results illustrated. In addition to this, cells migration was stimulated by the zinc-modified collagen porous scaffold due to zinc ions presence, enhancing thus the wound healing process in combination with the wild bilberry leaves extract in the scratch assay test.

The entrapment of the polyphenolic extract with high content of polyphenols and flavonoids into functionalized MSN carriers preserved the antioxidant properties of the free extract. The in vitro evaluation of the wild bilberry polyphenols encapsulated in functionalized MSN carriers showed good antimicrobial potential against both Gram-positive and Gram-negative bacterial strains, as well as anti-inflammatory activity, against LPS-induced inflammation, recommending the embedded extracts as strong immunomodulators. Furthermore, the growth of MelJuso tumor cells is inhibited after 72

h by the nanoconfined polyphenols in functionalized MSN, while there is a limited effect on the normal keratinocytes HaCaT cells after 72 h.

In summary, the designed novel composites arising from natural sources can be a useful tool in developing alternate wound dressings. These composites have potential for clinical translation in minor skin wounds treatment, to prevent potential bacterial infections and to stimulate tissue regeneration. The main advantage of these composites is that they can be available over the counter, without the requirement of a medical prescription. Furthermore, the use of naturally derived products offers the advantage of biodegradability of the composites, without raising other concerns, like their disposal after usage. Nature is a vast and complex source of bioactive substances that can become components in developing medical devices for wound healing. However, the development of such products requires standardized procedures for the assessment of these naturally derived products.

Acknowledgments

This work was conducted with the financial support of UEFISCDI National Funding Agency through project PCE no. 117/2022. The authors are thankful to the botanical specialist from National Institute for Chemical-Pharmaceutical Research & Development (INCDCF– ICCF Bucharest), Corina Bubueanu, for the identification of the plant material. This work involves plant material. No additional approvals were required to conduct research with plant material.

Disclosure

The authors report no conflicts of interest in this work.

References

1. Meng H, Zhao Y, Cai H. et al. Hydrogels containing chitosan-modified gold nanoparticles show significant efficacy in healing diabetic wounds infected with antibiotic-resistant bacteria. *Int J Nanomed.* 2024;19:1539–1556. doi:10.2147/IJN.S448282
2. Barakat HS, Freag MS, Gaber SM, Oufy A A, Abdallah OY. Development of Verapamil hydrochloride-loaded biopolymer-based composite electrospun nanofibrous mats: in vivo evaluation of enhanced burn wound healing without scar formation. *Drug Des Devel Ther.* 2023;17:1211–1231. doi:10.2147/DDDT.S389329
3. Liu X, Zheng C, Luo X, Wang X, Jiang H. Recent advances of collagen-based biomaterials: multi-hierarchical structure, modification and biomedical applications. *Mater Sci Eng C.* 2019;99:1509–1522. doi:10.1016/j.msec.2019.02.070
4. Sorushanova A, Delgado LM, Wu Z, et al. The collagen suprafamily: from biosynthesis to advanced biomaterial development. *Adv Mater.* 2019;31(1). doi:10.1002/adma.201801651
5. Yue C, Ding C, Su J, Cheng B. Effect of copper and zinc ions on type I collagen self-assembly. *Int J Polym Anal Charact.* 2022;27(6):394–408. doi:10.1080/1023666X.2022.2093569
6. Yu YY, Di FD. Coordination study of recombinant human-like collagen and zinc (II). *Spectrochim, Acta A Mol, Biomol, Spectrosc.* 2011;81(1):412–416. doi:10.1016/j.saa.2011.06.030
7. Dalisson B, Barralet J. Bioinorganics and wound healing. *Adv Healthc Mater.* 2019;8(18). doi:10.1002/adhm.201900764
8. Jin X, Shan J, Zhao J, et al. Bimetallic oxide Cu–Fe₃O₄ nanoclusters with multiple enzymatic activities for wound infection treatment and wound healing. *Acta Biomater.* 2024;173:403–419. doi:10.1016/j.actbio.2023.10.028
9. Jin X, Zhang W, Shan J, et al. Thermosensitive Hydrogel Loaded with Nickel-Copper Bimetallic Hollow Nanospheres with SOD and CAT Enzymatic-Like Activity Promotes Acute Wound Healing. *ACS Appl Mater Interfaces.* 2022;14(45):50677–50691. doi:10.1021/acsami.2c17242
10. Tapiero H, Tew KD. Trace elements in human physiology and pathology: zinc and metallothioneins. *Biomed Pharmacother.* 2003;57(9):399–411. doi:10.1016/S0753-3322(03)00081-7
11. Działo M, Mierziak J, Korzun U, Preisner M, Szopa J, Kulma A. The potential of plant phenolics in prevention and therapy of skin disorders. *Int J Mol Sci.* 2016;17(2). doi:10.3390/ijms17020160
12. Pop A, Berce C, Bolfa P, et al. Evaluation of the possible endocrine disruptive effect of butylated hydroxyanisole, butylated hydroxytoluene and propyl gallate in immature female rats. *Farmacia.* 2013;61:1.
13. Ștefănescu BE, Călinoiu LF, Ranga F, et al. Chemical composition and biological activities of the nord-west Romanian wild bilberry (*Vaccinium myrtillus* L.) and lingonberry (*Vaccinium vitis-idaea* L.) leaves. *Antioxidants.* 2020;9(6):495. doi:10.3390/antiox9060495
14. Ștefănescu R, Laczkó-Zöld E, Ősz BE, Vari CE. An updated systematic review of *Vaccinium myrtillus* leaves: phytochemistry and pharmacology. *Pharmaceutics.* 2023;15(1). doi:10.3390/pharmaceutics15010016
15. Ziemlewska A, Zagórska-Dziok M, Nizioł-lukaszewska Z. Assessment of cytotoxicity and antioxidant properties of berry leaves as by-products with potential application in cosmetic and pharmaceutical products. *Sci Rep.* 2021;11(1). doi:10.1038/s41598-021-82207-2
16. Tadić VM, Nešić I, Martinović M, et al. Old plant, new possibilities: wild bilberry (*Vaccinium myrtillus* L. Ericaceae) in topical skin preparation. *Antioxidants.* 2021;10(3):1–18. doi:10.3390/antiox10030465
17. Vaneková Z, Rollinger JM. Bilberries: curative and miraculous – a review on bioactive constituents and clinical research. *Front Pharmacol.* 2022;13. doi:10.3389/fphar.2022.909914
18. Debnath-Canning M, Unruh S, Vyas P, Daneshlatab N, Igamberdiev AU, Weber JT. Fruits and leaves from wild blueberry plants contain diverse polyphenols and decrease neuroinflammatory responses in microglia. *J Funct Foods.* 2020;68. doi:10.1016/j.jff.2020.103906

19. Tian Y, Puganen A, Alakomi HL, Uusitupa A, Saarela M, Yang B. Antioxidative and antibacterial activities of aqueous ethanol extracts of berries, leaves, and branches of berry plants. *Food Res Int.* 2018;106:291–303. doi:10.1016/j.foodres.2017.12.071
20. Han Y, Lin Z, Zhou J, et al. Polyphenol-mediated assembly of proteins for engineering functional materials. *Angewandte Chemie Int Ed.* 2020;59(36):15618–15625. doi:10.1002/anie.202002089
21. Ozdal T, Capanoglu E, Altay F. A review on protein-phenolic interactions and associated changes. *Food Res Int.* 2013;51(2):954–970. doi:10.1016/j.foodres.2013.02.009
22. Brezoiu AM, Matei C, Deaconu M, et al. Polyphenols extract from grape pomace. characterization and valorisation through encapsulation into mesoporous silica-type matrices. *Food and Chemical Toxicology.* 2019;133:110787. doi:10.1016/j.fct.2019.110787
23. Deaconu M, Prelipcean AM, Brezoiu AM, et al. Novel collagen-polyphenols-loaded silica composites for topical application. *Pharmaceutics.* 2023;15(2):312. doi:10.3390/pharmaceutics15020312
24. Brezoiu AM, Deaconu M, Mitran RA, Prelipcean AM, Matei C, Berger D. Optimisation of Polyphenols Extraction from Wild Bilberry Leaves—Antimicrobial Properties and Stability Studies. *Molecules.* 2023;28(15):5795. doi:10.3390/molecules28155795
25. Brezoiu AM, Lincu D, Deaconu M, Mitran RA, Berger D, Matei C. Enhanced stability of polyphenolic extracts from grape pomace achieved by embedding into mesoporous silica-type matrices. *UPB Sci Bull Series B.* 2020;82(3):3–20.
26. Neuenfeldt NH, Almeida Farias CA, de Oliveira Mello R, et al. Effects of blueberry extract co-microencapsulation on the survival of *Lactobacillus rhamnosus*. *LWT.* 2022;155. doi:10.1016/j.lwt.2021.112886.
27. Kropat C, Betz M, Kulozik U, et al. Effect of microformulation on the bioactivity of an anthocyanin-rich bilberry pomace extract (*Vaccinium myrtillus* L.) in vitro. *J Agric Food Chem.* 2013;61(20):4873–4881. doi:10.1021/jf305180j
28. Baum M, Schantz M, Leick S, et al. Is the antioxidative effectiveness of a bilberry extract influenced by encapsulation? *J Sci Food Agric.* 2014;94(11):2301–2307. doi:10.1002/jsfa.6558
29. Ge J, Yue P, Chi J, Liang J, Gao X. Formation and stability of anthocyanins-loaded nanocomplexes prepared with chitosan hydrochloride and carboxymethyl chitosan. *Food Hydrocoll.* 2018;74:23–31. doi:10.1016/j.foodhyd.2017.07.029
30. Todorović A, Šturm L, Salević-Jelić A, et al. Encapsulation of bilberry extract with maltodextrin and gum Arabic by freeze-drying: formulation, characterisation, and storage stability. *Processes.* 2022;10(10):1991. doi:10.3390/pr10101991
31. Ștefănescu BE, Nemes SA, Teleky BE, et al. Microencapsulation and bioaccessibility of phenolic compounds of *Vaccinium* leaf extracts. *Antioxidants.* 2022;11(4):674. doi:10.3390/antiox11040674
32. Kolisnyk TY, Ruban OA, Fil NY, Kutsenko SA. Application of an artificial neural network for design of sustained-release matrix tablets containing *Vaccinium myrtillus* leaf powder extract. *Asian J Pharm.* 2018;12(2):137–145. doi:10.22377/ajp.v12i02.2326
33. Deaconu M, Brezoiu AM, Mitran RA, et al. Exploiting the zwitterionic properties of lomefloxacin to tailor its delivery from functionalized MCM-41 silica. *Microporous Mesoporous Mater.* 2020;305:110323. doi:10.1016/j.micromeso.2020.110323
34. Arena P, Miceli N, Marino A, et al. Comparative study on phenolic profile and biological activities of the aerial parts of *Sinapis pubescens* L. subsp. *pubescens* (Brassicaceae) wild from Sicily (Italy). *Chem Biodivers.* 2023;20(6). doi:10.1002/cbdv.202300309
35. Sekhon-Loodu S, Rupasinghe HPV, Castanas E, Kampa M. Evaluation of antioxidant, antidiabetic and antiobesity potential of selected traditional medicinal plants. *Front Nutr.* 2019;6:6. doi:10.3389/fnut.2019.00053
36. Shan J, Jin X, Zhang C, et al. Metal natural product complex Ru-procyanidins with quadruple enzymatic activity combat infections from drug-resistant bacteria. *Acta Pharm Sin B.* 2024;14(5):2298–2316. doi:10.1016/j.apsb.2023.12.017
37. Tian H, Yan J, Zhang W, et al. Cu-GA-coordination polymer nanozymes with triple enzymatic activity for wound disinfection and accelerated wound healing. *Acta Biomater.* 2023;167:449–462. doi:10.1016/j.actbio.2023.05.048
38. Prelipcean AM, Iosageanu A, Gaspar-Pintilieșcu A, et al. Marine and agro-industrial by-products valorization intended for topical formulations in wound healing applications. *Materials.* 2022;15(10):3507. doi:10.3390/ma15103507
39. Brasanac-Vukanovic S, Mutic J, Stankovic DM, et al. Wild bilberry (*Vaccinium myrtillus* L. Ericaceae) from Montenegro as a source of antioxidants for use in the production of nutraceuticals. *Molecules.* 2018;23(8):1864. doi:10.3390/molecules23081864
40. Gil-Martínez L, Aznar-Ramos MJ, Del Carmen Razola-Díaz M, et al. Establishment of a sonotrode extraction method and evaluation of the antioxidant, antimicrobial and anticancer potential of an optimized *Vaccinium myrtillus* L. *Leaves Ext Func Ingre.* 2023;12(8). doi:10.3390/foods12081688
41. Liu P, Lindstedt A, Markkinen N, Sinkkonen J, Suomela JP, Yang B. Characterization of metabolite profiles of leaves of bilberry (*Vaccinium myrtillus* L.) and lingonberry (*Vaccinium vitis-idaea* L.). *J Agric Food Chem.* 2014;62(49):12015–12026. doi:10.1021/jf503521m
42. Bujor OC, Le bourvellec C, Volf I, Popa D, Dufour C. Seasonal variations of the phenolic constituents in bilberry (*Vaccinium myrtillus* L.) leaves, stems and fruits, and their antioxidant activity. *Food Chem.* 2016;213:58–68. doi:10.1016/j.foodchem.2016.06.042
43. Shraim AM, Ahmed TA, Rahman MM, Hijji YM. Determination of total flavonoid content by aluminum chloride assay: a critical evaluation. *LWT.* 2021;150. doi:10.1016/j.lwt.2021.111932
44. Xing L, Zhang H, Qi R, Tsao R, Mine Y. Recent advances in the understanding of the health benefits and molecular mechanisms associated with green tea polyphenols. *J Agric Food Chem.* 2019;67(4):1029–1043. doi:10.1021/acs.jafc.8b06146
45. Takács I, Szekeres A, Takács Á, et al. Wild strawberry, blackberry, and blueberry leaf extracts alleviate starch-induced hyperglycemia in prediabetic and diabetic mice. *Planta Med.* 2020;86(11):790–799. doi:10.1055/a-1164-8152
46. Bljajić K, Petlevski R, Vujić L, et al. Chemical composition, antioxidant and α -glucosidase-inhibiting activities of the aqueous and hydroethanolic extracts of *Vaccinium myrtillus* leaves. *Molecules.* 2017;22(5):703. doi:10.3390/molecules22050703
47. Xu L, Li W, Chen Z, et al. Inhibitory effect of epigallocatechin-3-O-gallate on α -glucosidase and its hypoglycemic effect via targeting PI3K/AKT signaling pathway in L6 skeletal muscle cells. *Int J Biol Macromol.* 2019;125:605–611. doi:10.1016/j.ijbiomac.2018.12.064
48. Li Z, Kang M, Zhang S, et al. The improved inhibition of Mn (II)-EGCG on α -glucosidase: characteristics and interactions properties. *J Mol Struct.* 2023;1283:135314. doi:10.1016/j.molstruc.2023.135314
49. Dai T, Li T, He X, et al. Analysis of inhibitory interaction between epigallocatechin gallate and alpha-glucosidase: a spectroscopy and molecular simulation study. *Spectrochim, Acta A Mol, Biomol, Spectrosc.* 2020;230. doi:10.1016/j.saa.2019.118023.
50. Liang JH, Lin HR, Yang CS, Liaw CC, Wang IC, Chen JJ. Bioactive components from *Ampelopsis japonica* with antioxidant, anti- α -glucosidase, and anticholinesterase activities. *Antioxidants.* 2022;11(7):1228. doi:10.3390/antiox11071228

51. Oboh G, Agunloye OM, Adefegha SA, Akinyemi AJ, Ademiluyi AO. Caffeic and chlorogenic acids inhibit key enzymes linked to type 2 diabetes (in vitro): a comparative study. *J Basic Clin Physiol Pharmacol.* 2015;26(2):165–170. doi:10.1515/jbcp-2013-0141
52. Li YQ, Zhou FC, Gao F, Bian JS, Shan F. Comparative evaluation of quercetin, isoquercetin and rutin as inhibitors of α -glucosidase. *J Agric Food Chem.* 2009;57(24):11463–11468. doi:10.1021/jf903083h
53. Ezzati N, Mahjoub AR, Abolhosseini Shahrnoy A, Syrgiannis Z. Amino Acid-functionalized hollow mesoporous silica nanospheres as efficient biocompatible drug carriers for anticancer applications. *Int J Pharm.* 2019;572. doi:10.1016/j.ijpharm.2019.118709
54. Alswieleh AM. Cysteine- and glycine-functionalized mesoporous silica as adsorbents for removal of paracetamol from aqueous solution. *Int J Environ Anal Chem.* 2023;103(9):2004–2015. doi:10.1080/03067319.2021.1887163
55. Ma J, Wang Z, Shi Y, Li Q. Synthesis and characterization of lysine-modified SBA-15 and its selective adsorption of scandium from a solution of rare earth elements. *RSC Adv.* 2014;40(78):41597–41604. doi:10.1039/c4ra07571d
56. Brodrecht M, Breitzke H, Gutmann T, Buntkowsky G. Biofunctionalization of nano channels by direct in-pore solid-phase peptide synthesis. *Chem a Eur J.* 2018;24(67):17814–17822. doi:10.1002/chem.201804065
57. Chaix A, Cueto-Diaz E, Delalande A, et al. Amino-acid functionalized porous silicon nanoparticles for the delivery of pDNA. *RSC Adv.* 2019;9(55):31895–31899. doi:10.1039/c9ra05461h
58. Parker FS. *Applications of Infrared Spectroscopy in Biochemistry, Biology, and Medicine.* In: Plenum Press; 1971:165–172.
59. Volf I, Ignat I, Neamtu M, Popa VI, Popa V. Thermal stability, antioxidant activity, and photo-oxidation of natural polyphenols. *Chem Papers.* 2014;68(1):121–129. doi:10.2478/s11696-013-0417-6
60. Choulitoudi E, Xristou M, Tsimogiannis D, Oreopoulou V. The effect of temperature on the phenolic content and oxidative stability of o/w emulsions enriched with natural extracts from *Satureja thymbra*. *Food Chem.* 2021;349. doi:10.1016/j.foodchem.2021.129206
61. Luo H, Lv XD, Wang GE, Li YF, Kurihara H, He RR. Anti-inflammatory effects of anthocyanins-rich extract from bilberry (*Vaccinium myrtillus* L.) on croton oil-induced ear edema and *Propionibacterium acnes* plus LPS-induced liver damage in mice. *Int J Food Sci Nutr.* 2014;65(5):594–601. doi:10.3109/09637486.2014.886184
62. Gato E, Perez A, Rosalowska A, Celeiro M, Bou G, Lores M. Multicomponent polyphenolic extracts from *Vaccinium corymbosum* at lab and pilot scale. Characterization and effectivity against nosocomial pathogens. *Plants.* 2021;10(12):2801. doi:10.3390/plants10122801
63. Mechikova GY, Kuzmich AS, Ponomarenko LP, et al. Cancer-preventive activities of secondary metabolites from leaves of the bilberry *Vaccinium smallii* A. *Gray Phyto Res.* 2010;24(11):1730–1732. doi:10.1002/ptr.3282
64. Ribera-Fonseca A, Jiménez D, Leal P, et al. The anti-proliferative and anti-invasive effect of leaf extracts of blueberry plants treated with methyl jasmonate on human gastric cancer in vitro is related to their antioxidant properties. *Antioxidants.* 2020;9(1):45. doi:10.3390/antiox9010045
65. Heldreth B, Bergfeld WF, Belsito D V, et al. Final report of the cosmetic ingredient review expert panel on the safety assessment of methyl acetate. *Int J Toxicol.* 2012;31(4_suppl):112S–136S. doi:10.1177/1091581812444142
66. Food and Drug Administration. CFR 347.10 skin protectant drug products for over-the-counter human use - active ingredients.; 2023. <https://www.ecfr.gov/current/title-21/part-347/section-347.10>. Accessed September 10, 2023.
67. Lansdown ABG. Interspecies variations in response to topical application of selected zinc compounds. *Food and Chemical Toxicology.* 1991;29(1):57–64. doi:10.1016/0278-6915(91)90063-D
68. Tenaud I, Saiagh I, Dreno B. Addition of zinc and manganese to a biological dressing. *J Dermatological Treat.* 2009;20(2):91–94. doi:10.1080/09546630802509089
69. Liu H, Wang S, Xi Y, Liu P. Preparation, characterization, and antibacterial activity evaluation of collagen-Zn complex. *Polym Bull.* 2010;64(8):835–843. doi:10.1007/s00289-009-0228-7
70. Meng K, Chen L, Xia G, Shen X. Effects of zinc sulfate and zinc lactate on the properties of tilapia (*Oreochromis Niloticus*) skin collagen peptide chelate zinc. *Food Chem.* 2021;347. doi:10.1016/j.foodchem.2021.129043
71. Barth A. Infrared spectroscopy of proteins. *Biochim Biophys Acta Bioenergy.* 2007;1767(9):1073–1101. doi:10.1016/j.bbabi.2007.06.004
72. Wu B, Mu C, Zhang GZ, Lin W. Effects of Cr 3+ on the Structure of Collagen Fiber. *Langmuir.* 2009;25(19):11905–11910. doi:10.1021/la901577j
73. Kraus TEC, Yu Z, Preston CM, Dahlgren RA, Zasoski RJ. Linking chemical reactivity and protein precipitation to structural characteristics of foliar tannins. *J Chem Ecol.* 2003;29(3):703–730. doi:10.1023/A:1022876804925
74. Liang CC, Park AY, Guan JL. In vitro scratch assay: a convenient and inexpensive method for analysis of cell migration in vitro. *Nat Protoc.* 2007;2(2):329–333. doi:10.1038/nprot.2007.30
75. Yang F, Xue Y, Wang F, et al. Sustained release of magnesium and zinc ions synergistically accelerates wound healing. *Bioact Mater.* 2023;26:88–101. doi:10.1016/j.bioactmat.2023.02.019
76. Wu G, Ma F, Xue Y, et al. Chondroitin sulfate zinc with antibacterial properties and anti-inflammatory effects for skin wound healing. *Carbohydr Polym.* 2022;278. doi:10.1016/j.carbpol.2021.118996
77. Vedhanayagam M, Unni Nair B, Sreeram KJ. Collagen-ZnO scaffolds for wound healing applications: role of dendrimer functionalization and nanoparticle morphology. *ACS Appl Bio Mater.* 2018;1(6):1942–1958. doi:10.1021/acsabm.8b00491